

UNIVERSITY OF OKLAHOMA
GRADUATE COLLEGE

STRATIGRAPHIC AND TEXTURAL ANALYSIS OF NANODIAMONDS ACROSS
THE YOUNGER DRYAS BOUNDARY SEDIMENTS OF WESTERN OKLAHOMA

A THESIS
SUBMITTED TO THE GRADUATE FACULTY
in partial fulfillment of the requirements for the
Degree of
MASTER OF SCIENCE

By
MOLLY REBECCA SEXTON
Norman, Oklahoma
2016

STRATIGRAPHIC AND TEXTURAL ANALYSIS OF NANODIAMONDS ACROSS
THE YOUNGER DRYAS BOUNDARY SEDIMENTS OF WESTERN OKLAHOMA

A THESIS APPROVED FOR THE
CONOCOPHILLIPS SCHOOL OF GEOLOGY AND GEOPHYSICS

BY

Dr. Andrew Elwood Madden, Chair

Dr. Megan Elwood Madden

Dr. Lee Bement

© Copyright by MOLLY REBECCA SEXTON 2016
All Rights Reserved.

Acknowledgements

I would like to thank my advisor, Andrew Elwood Madden, for his steadfast support. I would also like to thank the other members of my lab group for their insightful feedback. Greg Strout helped me for hours on end using the Transmission Electron Microscope. Lee Bement provided crucial information about the field site. I also appreciate the moral support of my friends and family.

Table of Contents

Acknowledgements	iv
List of Tables	vii
List of Figures.....	viii
Abstract.....	ix
Chapter 1. Introduction.....	1
Younger Dryas.....	1
The Younger Dryas Climate Event	1
Impact Hypothesis and Nanodiamonds	1
Other Evidence for an Impact.....	3
Nanodiamonds at Other Impact Events	3
Nanodiamond Textures and Their Implications	4
Raman Spectroscopy	6
Field Site.....	7
Chapter 2. Objectives and Hypotheses	9
Objectives	9
Hypotheses	9
Chapter 3. Methods	10
Selection of samples for nanodiamond analysis by TEM	10
Raman Spectroscopy	11
Transmission Electron Microscopy	12
Textural Analysis.....	12
Chapter 4. Results and Discussion	16

Raman spectroscopy	16
Results	16
Discussion.....	18
Transmission Electron Microscopy	19
Results	19
Discussion.....	20
Textural Analysis.....	22
Results	22
Discussion.....	23
References	26

List of Tables

Table 1. Samples examined using TEM.....	11
Table 2. Samples studied for textural analysis.....	13
Table 3. Results of textural analysis grouped by location.....	16
Table 4. Results of textural analysis grouped by age.	22
Table 5. Ratio analyses of textural analysis.	23

List of Figures

Figure 1. Map of the study area.....	8
Figure 2. Texture examples	14
Figure 3. Example of partial grains as possible twin.....	15
Figure 4. Raman data of commercial nanodiamonds on a muscovite substrate.....	17
Figure 5. Raman data of BC51 on different substrates.	18
Figure 6. TEM image of material with lattice fringes found in BC Clovis 22c.	19
Figure 7. TEM image of two nanodiamond-like objects found in BC Clovis 22c.....	20

Abstract

Exposed sediment profiles of the panhandle of western Oklahoma have previously been shown to contain two peak abundances of nanodiamonds, one dated approximately to the Younger Dryas and the other from the Late Holocene. The sediments of the Bull Creek Valley contain numerous Clovis culture artifacts and megafauna remains that disappeared after the Younger Dryas Boundary Layer. Firestone et al. have proposed that the reason for this sudden disappearance is a bolide impact that broke apart in the atmosphere, scattering debris across the world (2007). Nanodiamonds could be evidence for such an impact. In this study, I examined 12 additional samples collected at the same time as those reported by Bement et al. (2014) but not analyzed for nanodiamond content using Transmission Electron Microscopy (TEM). These samples were collected at various locations along the same Bull Creek valley, Oklahoma, including sediments older than those analyzed by Bement et al. (2014) and an additional nearby location that crosses the Younger Dryas Boundary. No nanodiamonds were found in these samples. However, the results may not be indicative of the true nanodiamond abundance. In a further test, a grid was prepared from a sediment digest solution shown by Bement et al. (2014) to have a peak abundance of nanodiamonds. No nanodiamonds were observed in this sample, suggesting that the nanodiamonds may have a finite lifetime when preserved in an ammonium hydroxide suspension. Additionally, Raman spectroscopy was investigated and ruled out as a means of screening samples for nanodiamond content more quickly and easily. Prepared samples of sediment solution previously confirmed to have nanodiamonds showed no Raman peaks associated with diamonds, though this could also have been the result of

the ammonium hydroxide suspension storage. However, samples of untreated commercial nanodiamonds also did not exhibit any characteristic diamond peaks, though possible peaks may have been obscured by heavy fluorescence.

Finally, the samples that were confirmed by Bement et al. (2014) to have nanodiamonds were divided into groups based on the ages of their sediments and high-resolution (HRTEM) images of them were examined for the textures of individual grains in order to gain a better insight of how they may have formed. The textures were categorized as having no lattice fringes, partial fringes, continuous fringes, linear twins, nonlinear twins, or star twins. The nanodiamond grains in the Younger Dryas Boundary group had the lowest ratio of linear to nonlinear grains and one of the highest ratios of star twins to twins, both of which are indicative of a chemical vapor deposition formation mechanism.

This is the first study to analyze and compare nanodiamond textures from the same stratigraphic area. The differences found between the older and younger nanodiamonds suggests that further studies comparing textures across spatial and temporal boundaries could lead to more definite signatures indicative of their origins.

Chapter 1. Introduction

Younger Dryas

The Younger Dryas Climate Event

The Younger Dryas climate event, which started about 13,000 years ago and lasted for approximately one thousand years, was a period of global cooling and glacier advancement that interrupted an otherwise warming progression of the Bølling-Allerød interstade and left behind a deposit of carbon-rich, black mats throughout the Northern hemisphere (Mahaney et al., 2013; Petaev et al., 2013). The Younger Dryas cooling is associated with the disappearance of the Clovis Culture and the extinction of most of the megafauna in North America, as remnants of both appear in the layer just below that of the Younger Dryas, but not within or above (Firestone et al. 2007). While there are many hypotheses for the cause of this cooling event and the subsequent extinctions, the scientific community lacks a consensus (e.g. Carlson, 2010; Firestone et al., 2007; Holliday et al., 2014; Petaev et al., 2013; Renssen et al., 2015; Wittke et al., 2013).

Impact Hypothesis and Nanodiamonds

An impact event has been proposed to be the cause of the climatic cooling during the Younger Dryas (e.g., Kennet et al., 2015; Kinzie et al., 2014). In support of this, a peak abundance level of nanodiamonds has been found in stratigraphic layers corresponding to the Younger Dryas boundary in several locations throughout the Northern Hemisphere, including in the Greenland Ice Sheet (Kinzie et al., 2014; Kurbatov et al., 2010). A possible impact event and the consequences thereof could explain the poorly understood extinction of the megafauna of North America and the

disappearance of the Clovis culture (Firestone et al., 2007). Positively identifying nanodiamonds in soil is very difficult and requires a great deal of sediment processing and imaging challenges, which means that the literature on the subject—and by association, our understanding of their place in the sedimentary record—is lacking. While nanodiamonds can be generated reproducibly in a laboratory setting, the processes that have been successful require lasers or detonation and therefore are unlikely to have contributed to the ancient geologic record (e.g., DeCarli and Jamieson, 1961; Peng et al., 2001; Kinzie et al., 2014).

Nanodiamond evidence for a Younger Dryas impact hypothesis was first proposed by Firestone et al. in 2007. Researchers opposed to this idea have suggested that the nanodiamonds formed entirely from terrestrial processes, such as wildfires or from Clovis hearths (e.g. Paquay et al., 2009), though other researchers maintain that forest fires do not reach high enough temperatures to form nanodiamonds (Bunch et al.; 2010). Daulton et al. attempted to replicate the nanodiamond results reported by Firestone et al. without success; however, they only analyzed crushed carbonaceous spherules from one site. In contrast, Bement et al. sampled entire sediment profiles from several different sites (2010; 2014) including those sampled by Kennet et al. (2009) and reproduced the YDB nanodiamond spike. Kloosterman et al. (2013) have suggested that scientists supporting the impact hypothesis did not actually sample the Younger Dryas boundary layer. Kennet et al. used Bayesian chronological modelling on 23 sediment profiles across the world to establish a date for the Younger Dryas Boundary that is consistent with the age of the sediments in which nanodiamonds have been found (2015). Bement et al. found nanodiamonds in the Bull Creek study area

with textures suggestive of an impact event; furthermore, they were unable to find nanodiamonds at the site of a Clovis culture hearth (2014).

Other Evidence for an Impact

In further support of the impact hypothesis, Bunch et al. found silica and iron-rich microspherules exclusively in sediment layers dated to the Younger Dryas whose geochemical signature appears to be similar to materials formed by cosmic impacts with Earth materials (2012). Mahaney et al. found similar results from their studies of a Younger Dryas layer in the Andes (2013). Petaev et al. found evidence for an impact in the form of a platinum peak corresponding to the Younger Dryas in Greenland Ice Sheet Project cores; they suggest that the impact could have been caused by a meteorite that had a high level of platinum and a low level of iridium (2013). Wittke et al. found about 10 million tons of carbon spherules scattered across approximately 50 million square kilometers in the northern hemisphere, which is consistent with other known impact strewnfields (2013).

Nanodiamonds at Other Impact Events

Nanodiamonds have been found to be associated with commonly established impact events as well. Carlisle & Braman found nanodiamonds in clay from the Cretaceous-Tertiary boundary after they treated the sediment with dissolution and oxidation procedures known to liberate nanodiamonds from some meteorites (1991). Gilmour et al. studied the isotope ratios of the K-T boundary nanodiamonds and found that their signatures more closely matched terrestrial signatures than cosmic signatures, hypothesizing that those nanodiamonds formed on Earth during the impact or resulting fireball (1992).

Nanodiamond Textures and Their Implications

Nanodiamond textures can give insight into how the nanodiamonds were formed. Daulton et al. studied nanodiamonds created in a lab setting using both shock detonation and chemical vapor deposition (CVD) methods in order to better understand how the nanodiamonds found in meteorites older than the solar system may have formed (1996). They observed by high-resolution transmission electron microscopy (HRTEM) that linear twins were far more common in the shock detonation diamonds, but that nonlinear and star twins dominated the CVD diamonds and the nanodiamonds in meteorites (Daulton et al., 1996). Shock detonation formation of nanodiamonds occurs when a carbon-rich material is hit hard enough to rearrange the atoms. CVD formation mechanisms involve atoms from a vapor cloud crystallizing directly into the new form. Kinzie et al. have suggested that the nanodiamonds observed in the Younger Dryas Boundary Layer could have formed from the vapor cloud around the fireball of a meteor passing through the atmosphere (2014). In support of this, the carbon isotopic signatures and carbon/nitrogen ratios of the carbon spherules suggest a terrestrial origin of the material (Tian et al., 2011).

Some of the textures observed in the Bull Creek valley study area similarly include fivefold star twins, strain fringes, linear twins, and nonlinear twins (Bement et al., 2014). Twinning refers to the phenomenon of multiple crystals sharing the same lattice plane. The fivefold symmetry of star twins in carbonaceous grains is unique to diamonds, although it can also be found in some metallic nanoparticles (Elwood Madden et al., 2013). Star twins and strain fringes were found in samples at the Bull Creek, Hearth, and Leavengood sites in the Bull Creek valley (Elwood Madden et al.,

2013). Linear and nonlinear twins differ in their twin boundaries, with parallel linear twins halting at the surface of the crystal and oblique nonlinear twins at the crystal surface or the intersections of the twins (Daulton et al, 1996). Linear twinning was found in samples at the Bull Creek site and nonlinear twinning was observed in samples from the Hearth and Leavengood sites (Elwood Madden et al., 2013). Star twins and nonlinear twins are characteristic of isotropic growth such as that found in chemical vapor deposition processes, whereas linear twins form from anisotropic growth such as that resulting from shock detonation (Daulton et al., 1996).

While all of the textures could correspond with the face centered cubic n-diamond phase of diamond, rather than the cubic phase; it has also been suggested that these features could also be consistent with cubic diamond (Cowley et al., 2004; Elwood Madden et al., 2013; Németh et al., 2015). The lattice fringes of the Bull Creek nanodiamonds that span whole crystals exhibit interplanar spacings and textures consistent with diamond phases, but not combinations of graphite, graphene, and graphene (Elwood Madden et al., 2013). One of the characteristic features of n-diamonds is that the electron scattering of the $\{100\}$ planes doesn't completely destructively interfere with the scattering of the $\{200\}$ planes so that the former is observable, in contrast to cubic diamonds in which the $\{100\}$ planes are absent from diffraction patterns (Cowley et al., 2004). However, Németh et al. have demonstrated that these forbidden zones can also be observed in regular cubic diamond in particularly thick samples or generated through additional sets of twins that are too difficult to observe using standard HRTEM methods (2015). Although one cannot definitively say whether the Bull Creek valley nanodiamonds and those reported by others are cubic or

'n-diamond', they are nonetheless present in the sediment samples with textures characteristic of chemical vapor deposition.

Kinzie et al. (2014) summarized nanodiamond presence and absence in Younger Dryas Boundary layers, and while they mentioned some details about textures, they did not perform a systematic analysis of the textures they found in different sites or different layers. Since nanodiamond textures are used to infer the conditions of their formation, more expansive research documenting nanodiamond textures could constrain the processes that contribute nanodiamonds to the sedimentary record throughout time. This study is the first step is the first step to filling that gap.

Raman Spectroscopy

Raman spectroscopy could potentially be a very useful tool for nanodiamond screening as it requires very little sample preparation and is mostly non-destructive (Nasdala et al., 2004). Currently, samples for nanodiamond analysis are screened using a lower resolution TEM before moving on to a high resolution TEM, in a process much like looking for a needle in a haystack. Raman has been used to study nanodiamonds collected from natural systems before; Kurbatov et al. used Raman spectroscopy to confirm that the nanodiamonds they found were n-diamond and not copper or rutile (2010). Raman spectroscopy could offer a much easier and faster alternative to indicative whether or not samples contain any nanodiamonds at all.

Since Raman is very sensitive to bonds, the sp^3 bonded C in diamond should be distinct from sp^2 -bonded carbon in graphite, graphene, and graphane (Mochalin et al., 2008). Diamond peaks occur around 1332 cm^{-1} , red-shifted in nanodiamonds due to their small size (Mermoux et al., 2014). Unfortunately, the cross-section for Raman

excitation of diamond bonds with most typical Raman excitation wavelengths is much smaller than that for most graphitic materials, so it is difficult to detect them (Osswald et al., 2006). Nanodiamond surfaces are also very sensitive to their environment. Heating, oxidation, etc. can lead to a surface coating of sp^2 -C that blocks the detection of the sp^3 carbon in the core of the particle (Cebik et al., 2013).

Field Site

All of the samples were taken from profiles along Bull Creek in the western Oklahoma panhandle (Figure 1) where there is an existing record of sediment that crosses the Younger Dryas Boundary. The samples were taken from multiple profiles in the area at different spatial locations, from which they are named. The samples are fluvial and aeolian sediments deposited in the Bull Creek valley during the Holocene (Arauzo et al., 2015).

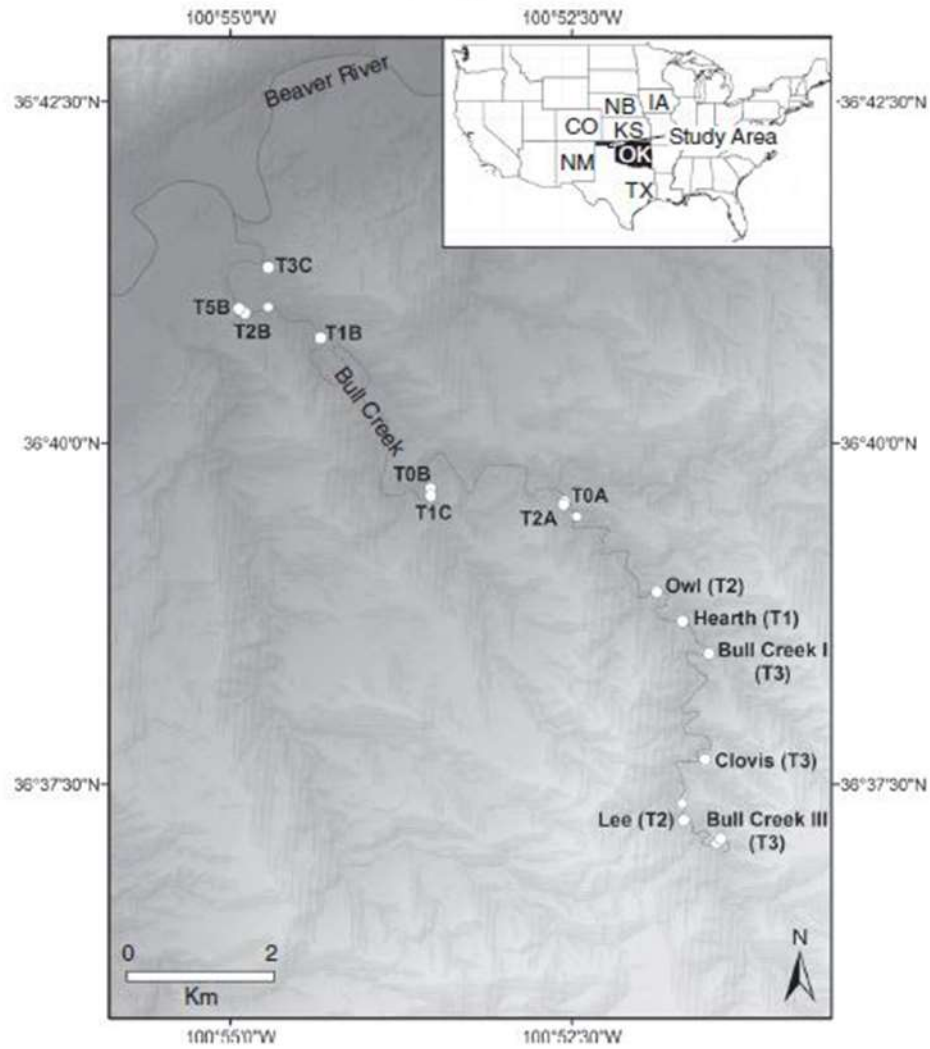


Figure 1. Map of the study area in western Oklahoma panhandle. This study focuses on the Bull Creek, Clovis, Hearth, Leavengood (Bull Creek III), and Beaver (not pictured) sites. The sites marked “T” are from the Arauza et al. study from which this map was taken (2015).

Chapter 2. Objectives and Hypotheses

Objectives

In this study, I investigate nanodiamonds (NDs) in the stratigraphic layer corresponding to and surrounding the Younger Dryas climate event in the Bull Creek area of western Oklahoma and compare the textures of the nanodiamonds to those that have already been found in the region. I also compare the nanodiamonds to see how the textures and distribution relate through time. Furthermore, I evaluate whether or not Raman spectroscopy is an efficient method to screen for nanodiamonds. Finally, I analyze the nanodiamonds found by Bement et al. and categorize them by texture (2014).

Hypotheses

I hypothesize that 1) there is a peak abundance of nanodiamonds throughout the Younger Dryas boundary layer in western Oklahoma that is not present in other layers; 2) that the nanodiamonds have isotropic textures associated with “defective” cubic structures thought to come from impact events; and 3) that the sediment samples dating to the Younger Dryas and Younger Dryas Boundary will have textures more closely associated with a CVD formation mechanism than the nanodiamonds in the younger sediments (Bement et al., 2014).

Chapter 3. Methods

Selection of samples for nanodiamond analysis by TEM

Bement et al. processed 71 sediment samples, all of which were analyzed for sediment properties and cultural artifacts (2014). However, only 48 of those samples were analyzed for nanodiamonds in their 2014 study. The 12 samples (Table 1) in this study come from the 23 sediment digestions that have not yet been examined for nanodiamonds. The samples include some from the same location, but different places within the vertical stratigraphic column (ranging from about 11,000 to 8200 radiocarbon years before present, which includes the Younger Dryas at about 10,900 RCYBP), and some from different spatial locations (Bement et al., 2014). The profiles from which the samples come have already been carefully studied for their sedimentological, archaeological, and soil science contexts; additionally, they have already been meticulously carbon dated.

Sample	¹⁴ C Yr BP	Cal. Yr BP
BC Clovis 23	9570 ± 50	10,720-11,130
BC Clovis 22d	10,280 ± 50	11,820-12,380
BC Clovis 22c	10,280 ± 50	11,820-12,380
BC Clovis 22b	10,280 ± 50	11,820-12,380
BC Clovis 22a	10,280 ± 50	11,820-12,380
BC Clovis 21	11,710 ± 70	13,390-13,750
BM1 3	26,880	31,705
BM1 4	27,940	32,426
BM1 5	38,160	42,538
BM2 4	25,800	30,838
BM2 5	26,080	31,010
BM2 6	>26,080	>31,010

Table 1. List of the samples, and their approximate ages, studied examined using Transmission Electron Microscopy. The ages for the BC Clovis samples came from Arauza et al. (2015). The BM sample ages are from personal communications with L. Bement.

Raman Spectroscopy

Samples of commercial nanodiamonds and BC51, which was already confirmed to have a peak abundance of nanodiamonds by Bement et al., were dropped in suspension onto various substrates after being in a sonic bath and analyzed using a Renishaw InVia scanning Raman spectrometer. A 532 nm laser was used to spot analyze at very low power levels (0.0001%) for 5 seconds and 5 accumulations at a time at a magnification of 50x in an attempt to prevent fluorescence or burning. Glass, quartz, silicon, and muscovite were all used as substrates since they were not expected to have peaks that might interfere with potential nanodiamond peaks.

Transmission Electron Microscopy

The samples were prepared for Transmission Electron Microscopy by centrifuging, at 3000 rpm for 30 minutes, a solution of the processed sample and water, in a 1:2 ratio, with a molybdenum TEM grid at the bottom of the tube. Afterwards, the grid was removed from the centrifuged solution and excess moisture was wicked away using a Kim wipe. It is necessary to use a molybdenum grid with ultrathin carbon film because the film is approximately the same thickness as the nanodiamonds and will therefore provide the minimum possible interference with energy dispersive spectroscopy (EDS) (Kinzie et al., 2014).

After preparing the grids, the samples were scanned for possible nanodiamond content by conventional TEM using a JEOL 2000FX TEM. At this stage, Energy Dispersive Spectroscopy (EDS) was also used to perform elemental analyses. While EDS can confirm the elemental composition of a sample, it cannot determine the structure or texture of a particle, and was therefore insufficient to identify nanodiamonds.

Samples that were thought to contain possible nanodiamonds were then examined using high resolution TEM (HRTEM) with a JEOL 2010F High Resolution TEM. At this stage, nanodiamond identification and texture analyses were possible.

Textural Analysis

Photographs of samples that were previously found to have a peak abundance of nanodiamonds by Bement et al. (Table 2) were studied and the lattice structures of the visible grains on each photograph were characterized by texture (2014). Each nanodiamond grain was classified into categories including “no fringes” for grains

where no lattice fringes were visible; “partial” for grains where only partial lattice fringes were visible; “continuous” for grains that had lattice fringes throughout the entire grain but did not have any twins; “linear” for grains that had a single twin or multiple linear twins; “nonlinear” for grains that had nonlinear twins; and “star twin” for grains that had the characteristic fivefold symmetry of star twins (Figure 2). The grains categorized as partials were assumed to be twins for analysis purposes because in some sets of photos, the same grain will appear to be partial in one photo and a twin in another (Figure 3); partial grains are very likely twinned grains of some sort that are oriented so that only part of the lattice structure can be seen at different focuses.

Sample	Depth (cmbs)	Age
BC52	0--10	Late Holocene
BC51	10--20	Late Holocene
BC38	134--144	PreBoreal/Atlantic
BC36	151--161	PreBoreal/Atlantic
BC35	161--171	PreBoreal/Atlantic
BC25	252--262	Younger Dryas
BC24	262--269	Younger Dryas
BC23	279--289	Younger Dryas
BC21	298--307	Younger Dryas Boundary
BC20	307--312	Younger Dryas Boundary
Hearth 22	100--110	Late Holocene
Hearth 19	132--142	Late Holocene
Hearth 17	153--164	Late Holocene
LEA19	302--310	Younger Dryas
LEA20	331--341	Younger Dryas Boundary
LEA22	387--399	Dansgaard-Oeschger

Table 2. Previously studied samples (that were confirmed to have nanodiamonds by Bement et al.), the depth at which they were taken (in centimeters below the surface), and their approximate ages (2014).

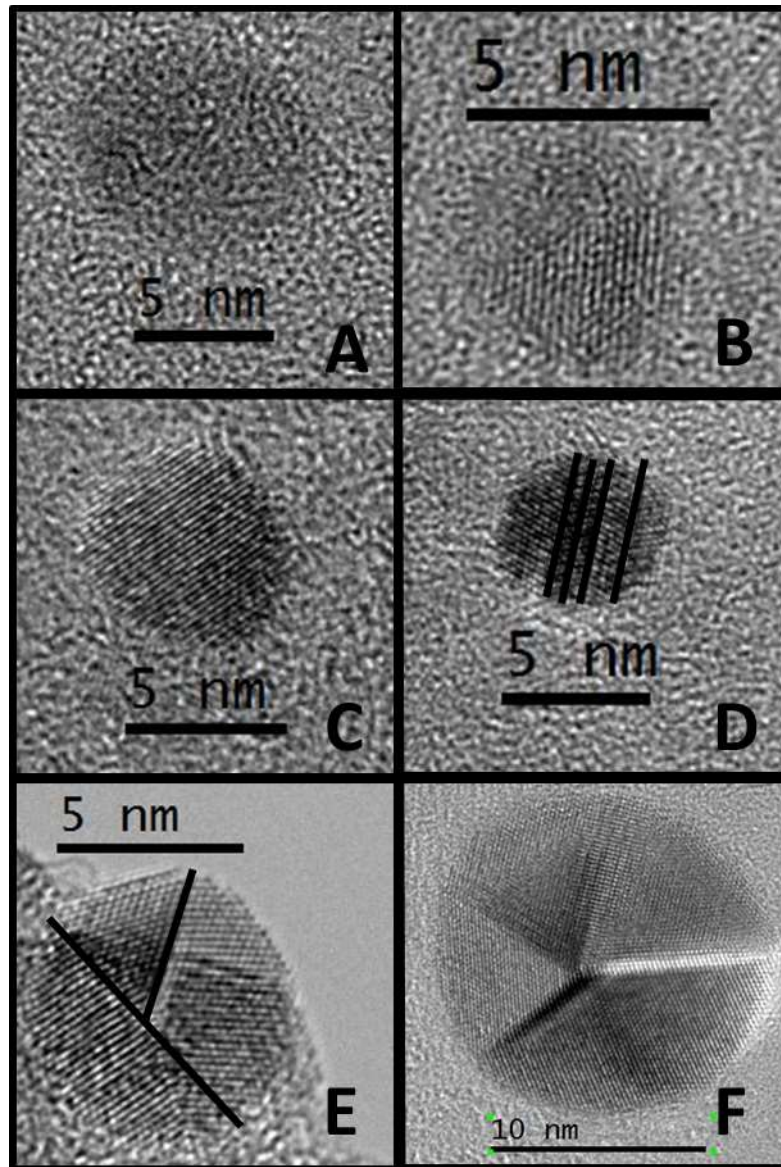


Figure 2. Texture examples. A is a grain with no lattice fringes from BC24; B is a grain with partial fringes from Hearth 17; C is a grain with continuous fringes from Hearth 22; D is a grain with linear twins from BC35; E is a grain with non-linear twins from BC52; F is a star twin from LEA19. The black lines on D and E indicate where the twin boundaries are.

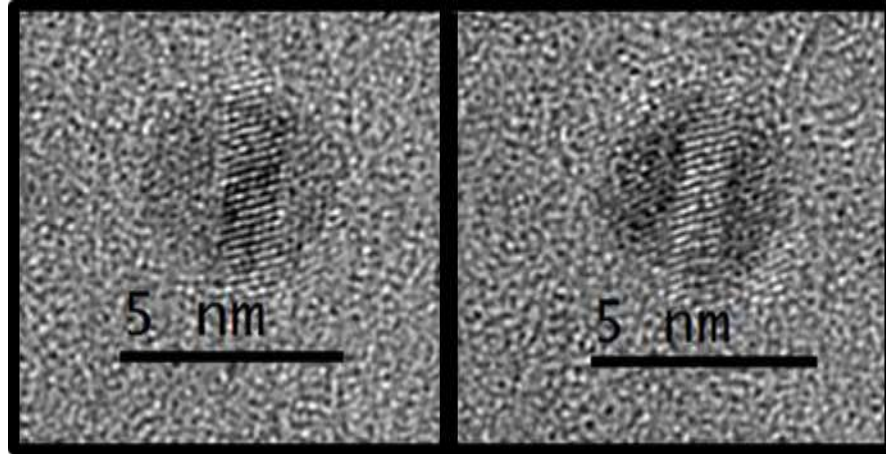


Figure 3. Two pictures of the same grain. The picture of the left would be categorized as a “partial” texture, whereas the picture on the right would be a linear twin.

The samples were first grouped by the locations within the Bull Creek Valley where they were collected. Then they were grouped by approximate age so that the Younger Dryas Boundary could be compared to other periods of time (Table 3). The time groupings were taken from the Bement et al. paper and include the Late Holocene (less than 3000 radiocarbon years before present), PreBoreal/Atlantic (a climatic aridity event about 9,850 RCYBP), the Younger Dryas (roughly 10,000 to 11,000 RCYBP), and the Younger Dryas Boundary (about 11,000 RCYBP) (2014).

Finally, following the example of Daulton et al., the ratios of linear twins to nonlinear twins, star twins to overall twins, and twins to single grains were calculated (1996). These ratios enable for better comparisons of different formation mechanism textures.

<u>Leavengood Samples</u>							
Sample	No Fringes	Partial	Continuous	Linear Twins	Non-linear Twins	Star Twins	Total
19	3	9	1	8	1	10	32
20	11	20	18	1	3	2	55
22	7	13	17	4	4	6	51
Total	21	42	36	13	8	18	138
<u>Hearth Samples</u>							
Sample	No Fringes	Partial	Continuous	Linear Twins	Non-linear Twins	Star Twins	Total
17	2	7	4	4	10	1	28
19	4	5	6	8	11	2	36
22	9	11	9	3	12	6	50
Total	15	23	19	15	33	9	114
<u>Bull Creek Samples</u>							
Sample	No Fringes	Partial	Continuous	Linear Twins	Non-linear Twins	Star Twins	Total
20	15	11	6	0	1	1	34
21	1	5	0	1	1	0	8
23	0	4	1	0	1	0	6
24	22	26	7	1	12	1	71
25	2	5	1	0	0	0	8
35	3	8	5	4	4	0	23
36	0	0	0	1	5	0	6
38	0	3	1	1	2	0	7
51	13	39	17	8	3	0	82
52	9	20	26	6	8	1	70
Total	65	121	64	22	37	3	315

Table 3. The results of the textural analysis for the previously studied samples, organized by location.

Chapter 4. Results and Discussion

Raman spectroscopy

Results

Commercial nanodiamonds were analyzed at very low power on a muscovite substrate, but no significant peaks were visible above the noise of the background (Figure 4). The sample BC 52, which was confirmed to have a high peak abundance of nanodiamonds by Bement et al., was also examined on substrates of muscovite, silicon, glass, and quartz (Figure 5) (2014). Again, no significant peaks were visible above the

background noise. Comparing the data from the four BC 52 samples also failed to identify any features common to all four samples. Commercial nanodiamonds were also analyzed on a muscovite substrate under the same conditions as the BC51 samples. The commercial nanodiamonds did not produce any significant peaks and instead produced too much fluorescence for the CCD.

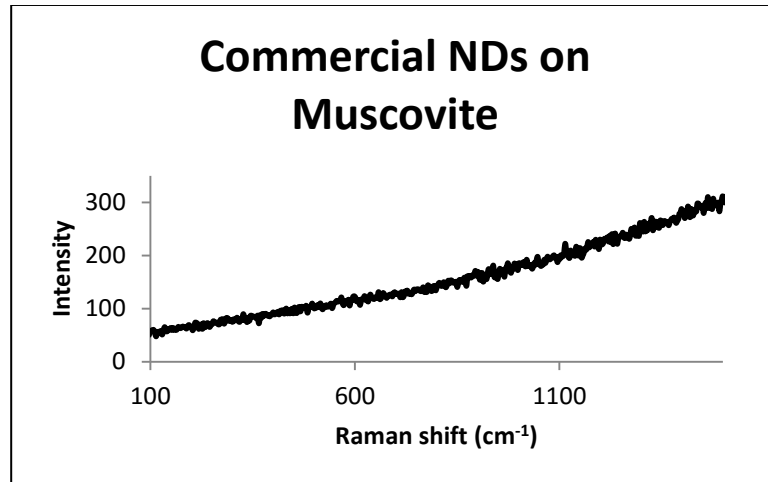


Figure 4. Commercial nanodiamonds on a muscovite substrate. No significant peaks were observed and the upward trend is due to fluorescence.

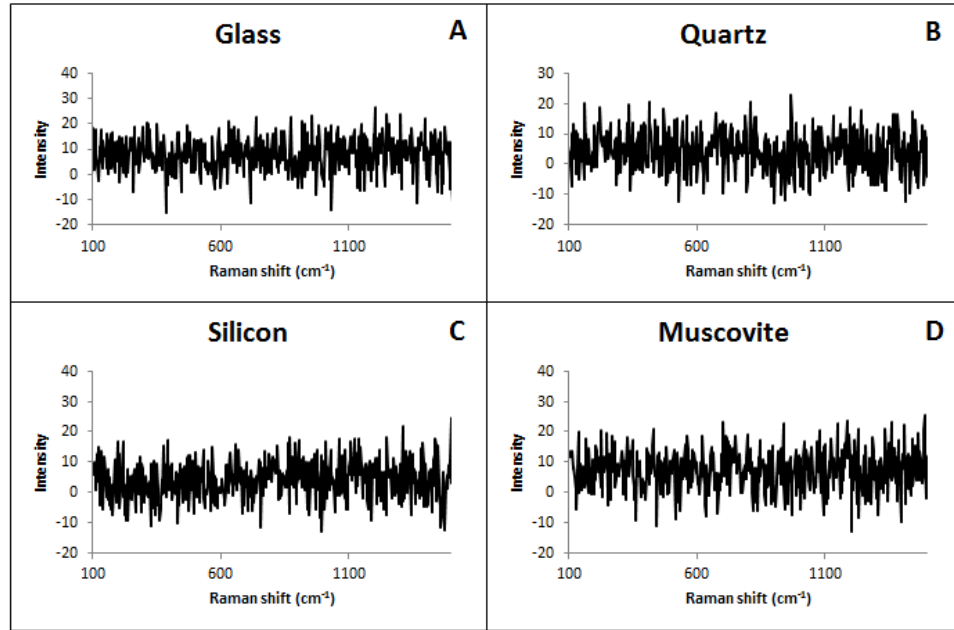


Figure 5. Raman results. Sample BC 51, which was confirmed to have nanodiamonds by Bement et al., on various substrates. A is a glass substrate; B is quartz; C is silicon; and D is muscovite. All the samples were run under the same Raman conditions. No significant Raman peaks were observed. The experimental conditions of the spectrometer were the same as for the commercial nanodiamonds.

Discussion

The nanodiamonds were not observable in any of the samples, even with commercial nanodiamonds and a sample that was already confirmed to have nanodiamonds. Most likely, the concentration of the nanodiamonds is too small to be detected by the Raman. However, trying to increase the power of the machine, the time for each measurement, or the number of captures per measurement all result in an excess of fluorescence that overwhelms the machine and produces data that trend upwards. Raman spectrometry is not currently a good method to use for screening for nanodiamond content.

Transmission Electron Microscopy

Results

The six samples from the Beaver site did not contain signs of nanodiamonds when scanned on the JEOL 2000FX TEM and therefore they were not examined under the JEOL 2010F High Resolution TEM. OF the six BC Clovis samples, only BC Clovis 22c contained signs of nanodiamonds. However, when this sample was analyzed under the high resolution TEM, it was shown to contain objects with lattice structure that were amorphous in shape, and therefore unlikely to be nanodiamonds (Figure 6). This sample did contain two small (~2nm) round objects that were identified as likely to be nanodiamonds, pending further analysis (Figure 7).

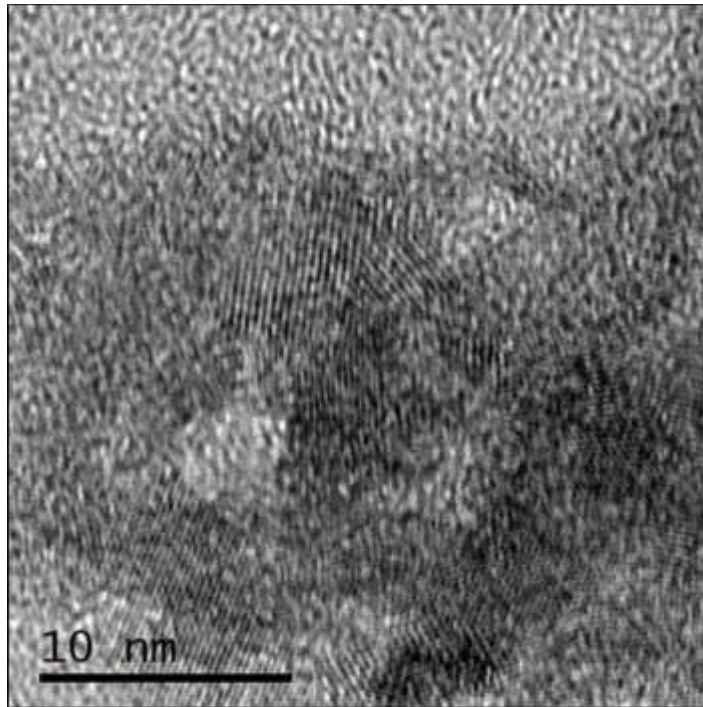


Figure 6. Objects with lattice fringes but without characteristic round shape, and are not likely to be nanodiamonds. Found in sample BC Clovis 22c.

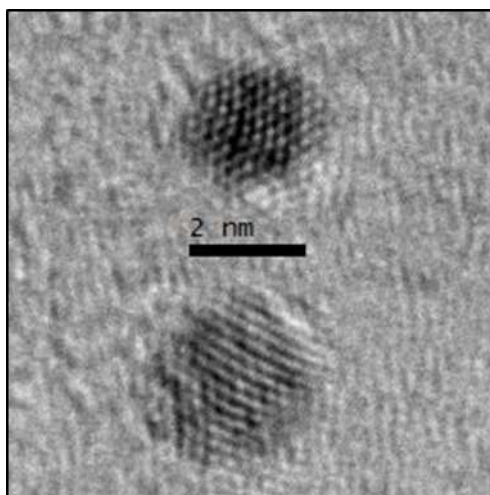


Figure 7. TEM image of the two nanodiamond-like objects found in BC Clovis 22c.

A new grid was prepared for BC 52, which had been confirmed to have nanodiamonds by Bement et al. (2014). Despite following the same preparation guidelines as used in the 2014 study, this BC 52 grid did not contain any nanodiamonds, though it did contain other carbonaceous material from the sediment digestion.

Discussion

None of the new samples were observed to contain any potential nanodiamonds for further analysis, with the exception of BC Clovis 22c. Further high-resolution analysis of BC Clovis 22c grains demonstrated that candidate grains were not nanodiamond. This sample had a great deal of matter that had lattice structure, but these grains were not in the characteristically round shape of nanodiamond and their d-spacings (2.3 Å and larger) were inconsistent with nanodiamonds (less than 2.1 Å at the largest). Two small, round objects (Figure 7) were consistent with the expected size and morphology of nanodiamonds, but their d-spacings (about 2.2 Å) were also larger than what has been observed for nanodiamonds. No other nanodiamond-like objects were

observed in the sample. Since these 12 samples were not from the Younger Dryas or Younger Dryas Boundary layer, this was to be expected.

A new TEM grid was prepared for sample BC52, which had previously been shown to contain a peak abundance of nanodiamonds by Bement et al. (2014). The same preparation methods that had been used by Bement et al. were used for this sample as well as all of the others, however no nanodiamonds were observed on this grid (2014). All of the sediment samples in this study, including the previously unanalyzed samples, were processed and stored in 2012, so it is possible that some sort of deterioration occurred in storage and it also is possible that the nanodiamond material stuck to the sides of the container while they sat in storage, and therefore did not make it onto the grid. However, the sample container was treated in an ultrasonic bath in order to dislodge material from the surface of the bottle.

Since no nanodiamonds were observed in the new BC52 grid, it is also possible that some sort of similar deterioration happened to the other samples and that they may once have been able to show nanodiamonds, though it is just as likely that those samples never contained nanodiamonds in the first place. Since the problem has not been identified, it cannot be said with certainty whether or not the new samples have or have ever had nanodiamonds. Furthermore, future studies should exercise caution with how they store their liquid samples; the TEM grids that were prepared in 2012 showed no deterioration, in contrast to the liquid sediment digests.

Textural Analysis

Results

Images that were taken of samples with high peak abundances of nanodiamonds in the Bement et al. study were analyzed in order to characterize the textures of the individual grains. The samples dating to the Late Holocene had the most overall grains with which to work; the Younger Dryas had the second largest amount of grains, and the Younger Dryas Boundary was third (Table 4).

Late Holocene							
Sample	No Fringes	Partial	Continuous	Linear Twins	Non-linear Twins	Star Twins	Total
BC 52	9	20	26	6	8	1	70
BC 51	13	39	17	8	3	0	82
Hearth 22	9	11	9	3	12	6	50
Hearth 19	4	5	6	8	11	2	36
Hearth 17	2	7	4	4	10	1	28
Totals	37	82	62	29	44	10	266
PreBoreal/Atlantic							
Sample	No Fringes	Partial	Continuous	Linear Twins	Non-linear Twins	Star Twins	Total
BC 38	0	3	1	1	2	0	7
BC 36	0	0	0	1	5	0	6
BC 35	3	8	5	4	4	0	23
Totals	3	11	6	6	11	0	36
Younger Dryas							
Sample	No Fringes	Partial	Continuous	Linear Twins	Non-linear Twins	Star Twins	Total
BC 25	2	5	1	0	0	0	8
BC 24	22	26	7	1	12	1	71
BC 23	0	4	1	0	1	0	6
Lea 19	3	9	1	8	1	10	32
Totals	27	44	10	9	14	11	117
Younger Dryas Boundary							
Sample	No Fringes	Partial	Continuous	Linear Twins	Non-linear Twins	Star Twins	Total
BC 21	1	5	0	1	1	0	8
BC 20	15	11	6	0	1	1	34
Lea 20	11	20	18	1	3	2	55
Totals	27	36	24	2	5	3	97
Other							
Sample	No Fringes	Partial	Continuous	Linear Twins	Non-linear Twins	Star Twins	Total
Lea 22	7	13	17	4	4	6	51

Table 4. Results of the textural analysis grouped by age.

The Younger Dryas Boundary nanodiamonds had the lowest ratio of linear to non-linear twins, significantly lower than the next lowest ratio of the Younger Dryas (Table 5). The Younger Dryas Boundary nanodiamonds had about the same ratio of star twins to twins as the Younger Dryas, both of which were relatively high. The Younger Dryas Boundary nanodiamonds also had by far the lowest ratio of twinned crystals to single crystals.

Time Period	Linear/Nonlinear	Star Twins/Twins	Twins/Single
Late Holocene	0.54	0.12	1.34
PreBoreal/Atlantic	0.55	0.00	2.83
Younger Dryas	0.36	0.32	3.40
Younger Dryas Boundary	0.25	0.30	0.42
LEA 22	0.40	0.43	0.82
Daulton et al. CVD	2.72	0.04	2.48
Daulton et al. Shock	0.36	0.23	1.48

Table 5. Ratios of linear to nonlinear twins, star twins to twin, and twins to single crystals for each age group. The Younger Dryas Boundary group has the lowest linear/nonlinear ratio by far, which is indicative of a CVD formation mechanism. CVD and shock detonation ratios taken from Daulton et al., 1996.

Discussion

Daulton et al.'s linear to nonlinear twin ratio was 2.72 for shock detonation and 0.36 for CVD; their ratios for star twins to twins was 0.04 and 0.23 for shock detonation and CVD respectively; and their ratios for twins to single crystals were 2.48 for shock detonation and 1.28 for CVD (1996).

For nanodiamonds investigated in this study, the Younger Dryas Boundary group has the lowest ratio of linear to nonlinear grain (0.25), though all of the age

groups have ratios closer to Daulton's value for CVD than for shock detonation. The Younger Dryas Boundary group also had a star twins/twins ratio of 0.30 that more closely matches Daulton et al.'s CVD ratio (1996). In this case, the Younger Dryas group and LEA 22 both have star twins/twins ratios more suggestive of CVD as well. The Late Holocene and PreBoreal/Atlantic both have low star twins/twins ratios like the shock detonation ratio. However, the presence of star twins in the Late Holocene may rule out shock detonation as a singular formation mechanism for those nanodiamonds, since they can only form isotropically (Daulton et al., 1996).

Finally, the Younger Dryas Boundary Layer group has by far the lowest ratio of twins to single crystals at 0.42, significantly lower than the ratios for both shock detonation and CVD. LEA 22 also has a small twins/single crystals ratio. The Late Holocene group's twins/single crystal ratio is the closest match to Daulton's CVD ratio. The PreBoreal/Atlantic group's twins/single crystal ratio most closely matches Daulton's shock detonation ratio. The Younger Dryas group's twins/single crystal ratio is significantly higher than Daulton's ratios for both shock detonation and CVD.

The Younger Dryas Boundary Layer group most closely matches a CVD formation mechanism, while the PreBoreal/Atlantic group most closely matches a shock detonation mechanism. The other groups fall somewhere in between, though they lean more closely to a CVD mechanism.

In order to better understand the relationship between nanodiamond textures and cosmic impact origins, it would be advisable to study the nanodiamonds found in the K-Pg impact layer. While nanodiamonds have been observed near the crater, their textures have not been analyzed to the extent of this study (Carlisle & Braman, 1991). It would

be especially helpful to note how the abundance and textures of nanodiamonds might change with proximity to the impact crater.

Other proposed origins of nanodiamonds include wildfires, lightning, and volcanism; though more research needs to be done to understand how these events might actually form nanodiamonds (Kinzie et al., 2014). The evidence for these alternative formation mechanisms is weak: fire does not get hot enough to form nanodiamonds without subsequently destroying them, nanodiamonds differ isotopically from cubic diamonds produced in the mantle, and no nanodiamonds have been found in fulgarites (Kinzie et al., 2014). Furthermore, it would be worthwhile to search for the process or processes that have produced nanodiamonds in the Late Holocene.

Anthropogenic processes, such as nuclear bomb detonations and coal-burning power plants, that would not have affected the older layers, could have played a role in the formation of these recent nanodiamonds. Additionally, there is an impact crater in Kansas that is less than a thousand years old that could have produced the nanodiamonds in the Late Holocene (Hodge, 1994).

It is important to note that the number of overall grains is highly variable between each group and that these initial ratios could very easily change with more available data. A large database of textural analyses from multiple spatial and temporal locations could be very useful for better understanding the link between textures and formation mechanisms.

References

- Arauzo, H. M., Simms, A. R., Bement, L. C., Carter, B. J., Conley, T., Woldergauy, A., ... Jaiswal, P. (2016). Geomorphic and sedimentary responses of the Bull Creek Valley (Southern High Plains, USA) to Pleistocene and Holocene environmental change. *Quaternary Research*, 85(1), 118–132.
<http://doi.org/10.1016/j.yqres.2015.11.006>
- Bement, L. C., Madden, A. S., Carter, B. J., Simms, A. R., Swindle, A. L., Alexander, H. M., ... Benamara, M. (2014). Quantifying the distribution of nanodiamonds in pre-Younger Dryas to recent age deposits along Bull Creek, Oklahoma Panhandle, USA. *Proceedings of the National Academy of Sciences*, 111(5), 1726–1731. <http://doi.org/10.1073/pnas.1309734111>
- Bunch, T. E., Hermes, R. E., Moore, A. M., Kennett, D. J., Weaver, J. C., Wittke, J. H., ... others. (2012). Very high-temperature impact melt products as evidence for cosmic airbursts and impacts 12,900 years ago. *Proceedings of the National Academy of Sciences*, 109(28), E1903–E1912.
- Carlisle, D. B., & Braman, D. R. (1991). Nanometre-size diamonds in the Cretaceous/Tertiary boundary clay of Alberta. *Nature*, 352(6337), 708–709.
<http://doi.org/10.1038/352708a0>
- Carlson, A. E. (2010). What Caused the Younger Dryas Cold Event? *Geology*, 38(4), 383–384. <http://doi.org/10.1130/focus042010.1>
- Cebik, J., McDonough, J. K., Peerally, F., Medrano, R., Neitzel, I., Gogotsi, Y., & Osswald, S. (2013). Raman spectroscopy study of the nanodiamond-to-carbon onion transformation. *Nanotechnology*, 24(20), 205703.
<http://doi.org/10.1088/0957-4484/24/20/205703>
- Cowley, J. M., Mani, R. C., Sunkara, M. K., O’Keeffe, M., & Bonneau, C. (2004). Structures of carbon nanocrystals. *Chemistry of Materials*, 16(24), 4905–4911.
- Daulton, T. L., Eisenhour, D. D., Bernatowicz, T. J., Lewis, R. S., & Buseck, P. R. (1996). Genesis of presolar diamonds: Comparative high-resolution transmission electron microscopy study of meteoritic and terrestrial nano-diamonds. *Geochimica et Cosmochimica Acta*, 60(23), 4853–4872.
- Daulton, T. L., Pinter, N., & Scott, A. C. (2010). No evidence of nanodiamonds in Younger–Dryas sediments to support an impact event. *Proceedings of the National Academy of Sciences*, 107(37), 16043–16047.
<http://doi.org/10.1073/pnas.1003904107>
- DeCarli P. S. and Jamieson J. C. (1961) Formation of Diamond by Explosive Shock. *Science* 133, 1821–1822.

- Elwood Madden AS, Bement LC, Carter B, Simms A, Swindle AL, Alexander HM, Fine S, Benemara M (2013) Nanodiamond quantification in pre-Younger Dryas to recent age deposits along Bull Creek, Oklahoma, USA, Geological Society of America Annual Meeting abstract. Ferrari, A. C., & Robertson, J. (2004). Raman spectroscopy of amorphous, nanostructured, diamond-like carbon, and nanodiamond. *Philosophical Transactions of the Royal Society A: Mathematical, Physical and Engineering Sciences*, 362(1824), 2477–2512. <http://doi.org/10.1098/rsta.2004.1452>
- Firestone, R. B., West, A., Kennett, J. P., Becker, L., Bunch, T. E., Revay, Z. S., ... others. (2007). Evidence for an extraterrestrial impact 12,900 years ago that contributed to the megafaunal extinctions and the Younger Dryas cooling. *Proceedings of the National Academy of Sciences*, 104(41), 16016–16021.
- Gilmour, I., Russell, S. S., Arden, J. W., Lee, M. R., Franchi, I. A., & Pillinger, C. T. (1992). Terrestrial Carbon and Nitrogen Isotopic Ratios from Cretaceous-Tertiary Boundary Nanodiamonds. *Science*, 258(5088), 1624–1626. <http://doi.org/10.1126/science.258.5088.1624>
- Gouadec, G., & Colomban, P. (2007). Raman Spectroscopy of nanomaterials: How spectra relate to disorder, particle size and mechanical properties. *Progress in Crystal Growth and Characterization of Materials*, 53(1), 1–56. <http://doi.org/10.1016/j.pcrysgrow.2007.01.001>
- Hodge, P. (1994). *Meteorite craters and impact structures of the Earth*. Cambridge University Press.
- Holliday V. T., Surovell T., Meltzer D. J., Grayson D. K. and Boslough M. (2014) The Younger Dryas impact hypothesis: a cosmic catastrophe. *Journal of Quaternary Science* 29.6, 515–530.
- Kennett, D. J., Kennett, J. P., West, A., Mercer, C., Hee, S. S. Q., Bement, L., ... Wolbach, W. S. (2009). Nanodiamonds in the Younger Dryas Boundary Sediment Layer. *Science*, 323(5910), 94–94. <http://doi.org/10.1126/science.1162819>
- Kennett, J. P., Kennett, D. J., Culleton, B. J., Aura Tortosa, J. E., Bischoff, J. L., Bunch, T. E., ... West, A. (2015). Bayesian chronological analyses consistent with synchronous age of 12,835–12,735 Cal B.P. for Younger Dryas boundary on four continents. *Proceedings of the National Academy of Sciences*, 112(32), E4344–E4353. <http://doi.org/10.1073/pnas.1507146112>
- Kinzie, C. R., Que Hee, S. S., Stich, A., Tague, K. A., Mercer, C., Razink, J. J., ... Wolbach, W. S. (2014). Nanodiamond-Rich Layer across Three Continents

Consistent with Major Cosmic Impact at 12,800 Cal BP. *The Journal of Geology*, 122(5), 475–506. <http://doi.org/10.1086/677046>

- Kloosterman J. B., Revay Z., Howard G. A., Kimbel D. R., Kletetschka G., Nabelek L., Lipo C.P., Sakai S., West A. and Firestone R. B. (2013) Evidence for deposition of 10 million tonnes of impact spherules across four continents 12,800 y ago. *Proceedings of the National Academy of Sciences* 110, E2088–E2097.
- Kurbatov, A. V., Mayewski, P. A., Steffensen, J. P., West, A., Kennett, D. J., Kennett, J. P., ... others. (2010). Discovery of a nanodiamond-rich layer in the Greenland ice sheet. *Journal of Glaciology*, 56(199), 747–757.
- Mahaney, W. C., Keiser, L., Krinsley, D., Kalm, V., Beukens, R., & West, A. (2013). New Evidence from a Black Mat Site in the Northern Andes Supporting a Cosmic Impact 12,800 Years Ago. *The Journal of Geology*, 121(4), 309–325. <http://doi.org/10.1086/670652>
- Mermoux, M., Crisci, A., Petit, T., Girard, H. A., & Arnault, J.-C. (2014). Surface Modifications of Detonation Nanodiamonds Probed by Multiwavelength Raman Spectroscopy. *The Journal of Physical Chemistry C*, 118(40), 23415–23425. <http://doi.org/10.1021/jp507377z>
- Mochalin, V., Osswald, S., & Gogotsi, Y. (2009). Contribution of Functional Groups to the Raman Spectrum of Nanodiamond Powders. *Chemistry of Materials*, 21(2), 273–279. <http://doi.org/10.1021/cm802057q>
- Nasdala, L. U. T. Z., Smith, D. C., Kaindl, R. E. I. N. H. A. R. D., & Ziemann, M. A. (2004). Raman spectroscopy: analytical perspectives in mineralogical research. *Spectroscopic methods in mineralogy*, 6, 281–343.
- Németh, P., Garvie, L. A. J., Aoki, T., Dubrovinskaia, N., Dubrovinsky, L., & Buseck, P. R. (2014). Lonsdaleite is faulted and twinned cubic diamond and does not exist as a discrete material. *Nature Communications* 5. Retrieved from <http://dx.doi.org/10.1038/ncomms6447>
- Osswald, S., Yushin, G., Mochalin, V., Kucheyev, S. O., & Gogotsi, Y. (2006). Control of sp²/sp³ Carbon Ratio and Surface Chemistry of Nanodiamond Powders by Selective Oxidation in Air. *Journal of the American Chemical Society*, 128(35), 11635–11642. <http://doi.org/10.1021/ja063303n>
- Paquay, F. S., Goderis, S., Ravizza, G., Vanhaeck, F., Boyd, M., Surovell, T. A., ... Claey, P. (2009). Absence of geochemical evidence for an impact event at the Bølling–Allerød/Younger Dryas transition. *Proceedings of the National Academy of Sciences*, 106(51), 21505–21510. <http://doi.org/10.1073/pnas.0908874106>

- Peng, J. L., Bursill, L. A., Jiang, B., Orwa, J. O., & Prawer, S. (2001). Growth of c-diamond, n-diamond and i-carbon nanophases in carbon-ion-implanted fused quartz. *Philosophical Magazine Part B*, 81(12), 2071–2087. <http://doi.org/10.1080/13642810108208558>
- Petaev, M. I., Huang, S., Jacobsen, S. B., & Zindler, A. (2013). Large Pt anomaly in the Greenland ice core points to a cataclysm at the onset of Younger Dryas. *Proceedings of the National Academy of Sciences*, 110(32), 12917–12920. <http://doi.org/10.1073/pnas.1303924110>
- Renssen, H., Mairesse, A., Goosse, H., Mathiot, P., Heiri, O., Roche, D. M., ... Valdes, P. J. (2015). Multiple causes of the Younger Dryas cold period. *Nature Geoscience*, 8(12), 946–949.
- Tian, H., Schryvers, D., & Claeys, P. (2011). Nanodiamonds do not provide unique evidence for a Younger Dryas impact. *Proceedings of the National Academy of Sciences*, 108(1), 40–44. <http://doi.org/10.1073/pnas.1007695108>
- Wittke, J. H., Weaver, J. C., Bunch, T. E., Kennett, J. P., Kennett, D. J., Moore, A. M., ... others. (2013). Evidence for deposition of 10 million tonnes of impact spherules across four continents 12,800 y ago. *Proceedings of the National Academy of Sciences*, 110(23), E2088–E2097.